SCR-64-84

SANDIA CORPORATION

REPRINT

# A HIGH-ENERGY SHOCK FACILITY USING ELECTROMAGNETIC ENERGY

Thomas F. Meagher

August 1964

# A HIGH-ENERGY SHOCK FACILITY USING ELECTROMAGNETIC ENERGY

By: Thomas F. Meagher, Sandia Corp. Livermore Laboratory

Thomas F. Meagher

Mr. Meagher has been employed by Sandia Corporation, Livermore Laboratory, since his graduation with a BSEE degree from the University of Washington in 1960. He has been responsible for dynamic and climatic tests, has established an electrical-measurement laboratory, and during the past 3 years has been working on the design of various special test facilities, including a facility for the conversion of electromagnetic energy into mechanical shock pulses. He is a member of the IES and is presently working on an advanced degree in Applied Science.

## Abstract

The repulsion-coil technique for energy conversion offers a powerful, new tool in the field of acceleration testing. Using this technique, a prototype magnetic shock device was developed that uses electrical energy stored in a capacitor bank to produce high-g, mechanical acceleration pulses.

A disc projectile is vacuum-held against the core of an electromagnet coil and a crystal accelerometer is attached to the projectile to monitor the pulse. The capacitor bank is charged to a specific voltage between one and 20 kv, then discharged into the coil. The resultant magnetic field around the coil effects a repulsion of the projectile, which is mechanically free to move away from the coil. By varying the capacitor voltage, the magnitude of the pulse can be predicted and controlled.

This investigation is intended to demonstrate the application of electrical-energy conversion in the production of a controllable acceleration pulse, toward development of a magnetic shock device for component testing and instrument calibration.

## Introduction

This report describes an investigation into the properties and use of stored electrical energy and its conversion to mechanical energy. The investigation stems from a need at Sandia Corporation, Livermore Laboratory, for a mechanical shock-test facility capable of controlled acceleration magnitude and duration, covering the range of 100,000-g acceleration with a 100 microsecond duration, to a 20,000-g pulse with a one-millisecond duration (assuming a one-pound test package).

This report provides the theory, description, and test results of a prototype shock device, based on a theory of electromagnetic repulsion, using electrical energy stored in a capacitor bank.

Primary requirements for a sophisticated test device were determined to be:

1. Variable-acceleration pulse amplitude and width
2. Repeatable acceleration signature
3. Freedom from mechanical noise

Forces attainable from high-magnitude, transient, magnetic fields have been used in a variety of ways, most notably in plasma "pinch" experiments. Industry uses transient magnetic fields in many metal-forming applications requiring high force. It was determined that these same forces could be used to produce high-g, mechanical acceleration pulses.

## Theory

Primary elements of the magnetic shock device (Figure 1) include electrical energy stored in capacitor banks and the repulsion coil mounted in the test enclosure. Basic principles involve the conversion of the energy stored in the capacitors into mechanical kinetic energy. Energy is converted by discharging the capacitor bank through the coil, which creates a time-varying magnetic field. The field reacts against a conductor (projectile) located close to the coil windings causing the projectile to accelerate away from the coil.

To determine the force of acceleration on the moving projectile, three basic theoretical approaches are available: circuit theory, field energy theory, and field analysis theory. These three theories are developed in detail in Appendixes A, B, and C respectively. However, a brief discussion of the theory of electromagnetic repulsion is included below.

### Electromagnetic Repulsion

In general, if a conducting material is placed in the presence of a time-varying magnetic field, a current flow will be induced in the conducting material. If the period, or pulse time, of the magnetic field is short enough, all the induced current will be concentrated on or near the surface of the conducting material. The reaction between the surface current and the magnetic field creates a force of repulsion that causes the conductor to accelerate away from the magnetic field. If the geometry of the system ensures that the magnetic field is present on only one side of the conductor, then a net accelerating force is developed and the conductor, if free to move, becomes a projectile.

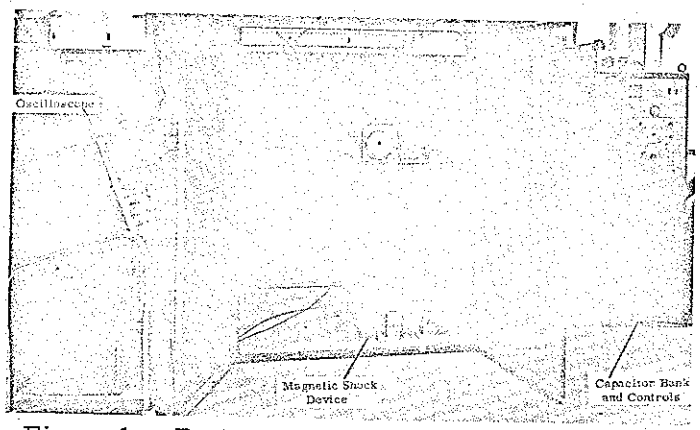


Figure 1. Prototype Magnetic Shock Device

The force developed on the conductor may be expressed in several ways. In terms of the magnetic field density existing at the surface of the conductor, the force per unit area, or magnetic pressure, is expressed in Gaussian units, as

$$P = \frac{B^2}{8\pi} \qquad (1)$$

where P is the magnetic pressure and B is the magnetic flux density. If the system is considered a mutually coupled inductive circuit, the force is expressed in MKS units, as

$$F = i_1 \, i_2 \, \frac{\partial M}{\partial X} \qquad (2)$$

where F is the accelerating force, $i_1$ is the current in the primary, $i_2$ is the current in the secondary, and $\frac{\partial M}{\partial X}$ is the rate of change of mutual inductance with respect to distance.

## Description

The prototype unit was designed primarily to demonstrate the feasibility of using the energy available from high-magnitude, transient, magnetic fields.

Energy-Storage Component -- The energy storage component was a 24,000-joule, 120-farad capacitor bank, complete with power supply and operating controls. The power supply was a modified 5-KVA distribution transformer fed by a 208-volt, single-phase source. The transformer output was fed through a voltage doubler to a peak rectifying circuit. Electrical energy was stored in eight 14.5-farad capacitors rated at 20 KV each, of the standard chlorinated diphenyl energy storage type. The capacitor bank was switched through standard size D ignitrons. It was completely enclosed as a unit and was mounted on casters.

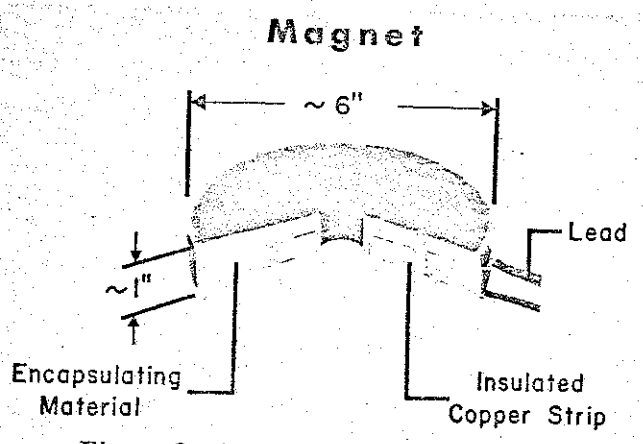


Figure 2. Typical Pancake Coil

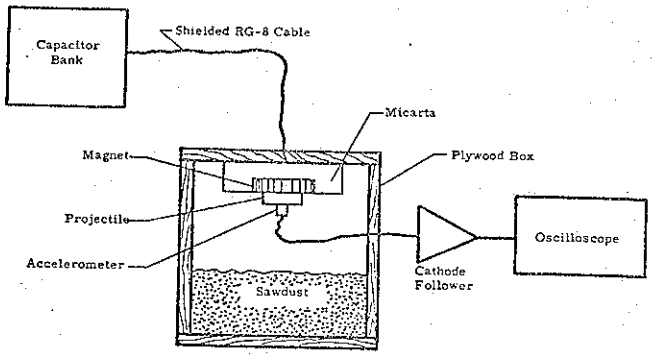


Figure 3. Simplified Diagram of Test Setup

Magnets -- Two types of flat, circular magnets were used to produce the time-varying magnetic fields. The first type was a flat spiral (pancake) coil consisting of 30 turns of 0.5-inch by 0.03-inch copper strip separated by glass tape. The entire winding was encapsulated in a dielectric compound so that the edge of the copper winding was from 0.03 inch to 0.12 inch from the face of the coil assembly, depending on the actual thickness of the compound. The inner diameter of the winding was about 1-3/8 inches, and the outer diameter was from 4 to 4-1/2 inches. These coils had self-inductances ranging from 40 to 65 microhenries, depending on the coil. The entire magnet assembly was about 1 inch thick. (Figure 2 shows a typical pancake coil.) In addition to the pancake magnets

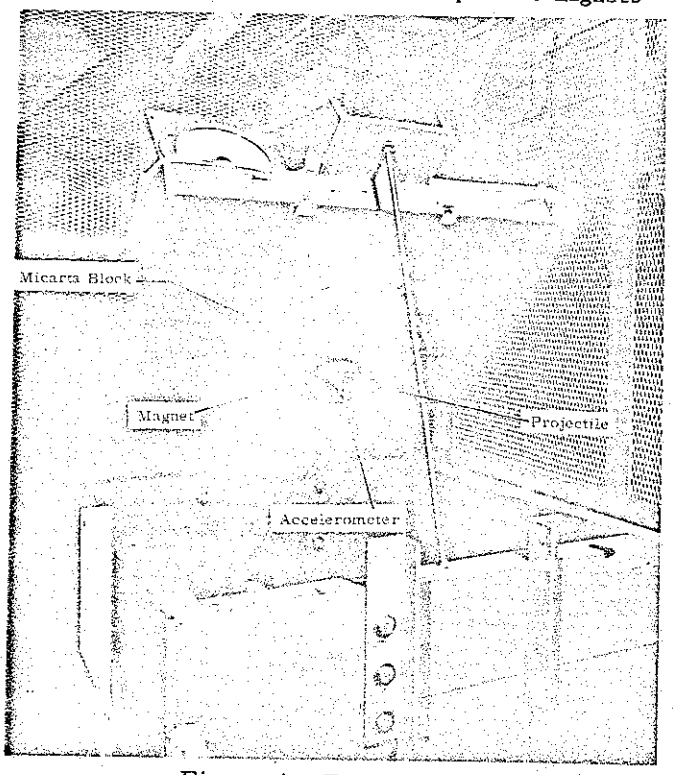


Figure 4. Test Setup

described above, coils fabricated from round wire were used. These coils had approximately the same volume of winding space but consisted of 100 turns of #10 wire, 200 turns of #12 wire, and 300 turns of #14 wire. Standard Formvar magnet wire was used, with mylar strip insulation between layers. As will be seen later, the main purpose of these coils was to increase the acceleration pulse time by raising the coil inductance.

Projectiles -- Disc-shaped projectiles of various sizes were used; diameters varied between 1 and 4-1/2 inches and thicknesses varied between 1 and 3 inches. The larger diameter projectiles received a greater accelerating force, but were more easily excited into an undesirable resonant condition. Most of the projectiles used were fabricated from aluminum, although beryllium was used in some instances. (Although beryllium is less susceptible to resonant excitation because of its greater stiffness, it is much more expensive and difficult to machine.)

Accelerometers -- Piezoelectric crystal accelerometers were mounted directly to the projectile in such a manner that no mechanical filtering was present. Projectile acceleration was monitored in the center of the disc, away from the coil (see Figure 3). The projectile was held against the disc by a vacuum through the center of the coil. The accelerometer cable hung from the projectile, and the accelerometer output was fed through a cathode follower to an oscilloscope with a Polaroid camera attachment. The high frequency response of the transducer and recording system prevented any electronic filtering.

Test Unit Configuration -- The magnet was placed in a micarta block and bolted to the underside of the enclosure top (see Figure 4). The 2-inch thick plywood enclosure was filled with sawdust to within 18-24 inches of the disc. The capacitor bank was connected in parallel to the magnet through four shielded RG-8 cables.

## Application

Figure 5 shows a cross-section representation of the current and field relationship of the magnet and the projectile. When the projectile is close to the winding, the flux lines are essentially parallel to the projectile surface. However, the flux lines bend away from the projectile surface near the center of the projectile, resulting in a decreasing pressure in that area.

## Operation

The projectile is vacuum-held against the magnet. After the projectile is in place, a vacuum switch is closed to charge the capacitors. The capacitor voltage is then monitored through a metering circuit that causes the vacuum switch to open when the desired capacitor voltage has been reached (see Figure 6). Since at this point the ignitrons are in a nonconducting state, voltage is locked on the capacitors. When the selected voltage is reached, the capacitors are discharged through the coil by converting Ignitron 1 to a conducting state. This is accomplished by sending an "ignite" pulse simultaneously to the ignitron and to a time-delay pulse generator. The current in the magnet rises sinusoidally until the quarter-

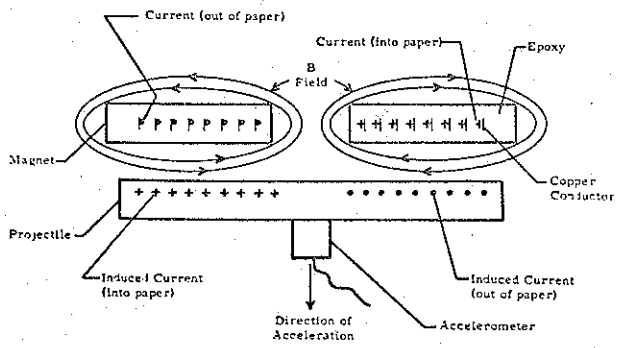


Figure 5. Cross-Section Showing Current and Field Relationship of Magnet and Projectile

cycle peak is reached, then the preset time-delay pulse generator ignites Ignitron 2. The magnet is then short-circuited (crowbarred) through Ignitron 2 and $R_{cb}$. The short-circuiting operation maintains the direction of the current flow, which then attenuates exponentially as described by the $L/R_{cb}$ time constant of the shorted circuit. The field generated by the magnet repels the projectile.

## Efficiency

The energy contained in a magnetic field is given by:

$$\text{Energy} = \frac{1}{2} LI^2, \tag{3}$$

and the total flux contained is:

$$\emptyset = LI \tag{4}$$

where L is the inductance of the field producing coil, I is the current flowing in the coil and $\emptyset$ is the total flux produced by the coil. From an electrical system energy viewpoint, H. P. Furth (Reference 1) has shown that the maximum energy efficiency, up to the time of peak current, that may be realized is:

$$\epsilon < \frac{\Delta L}{L_o + 2\Delta L} \tag{5}$$

If the current is brought very rapidly to its maximum value and the coil is short-circuited, the energy efficiency becomes:

$$\epsilon < \frac{\Delta L}{L_o + \Delta L} \tag{6}$$

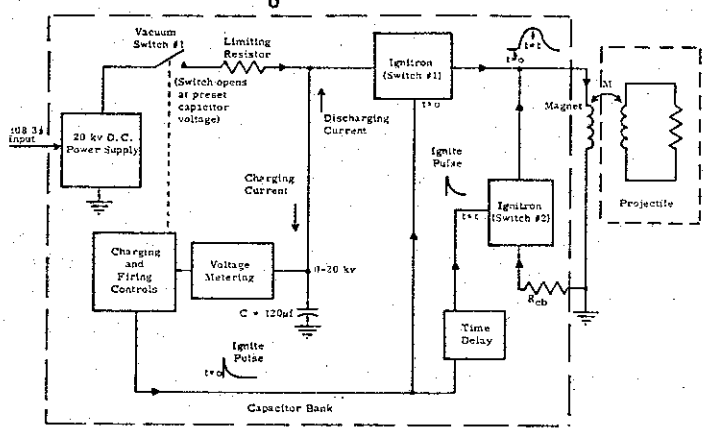


Figure 6. Block Diagram of Capacitor Bank and Controls

where $\Delta L$ is the inductance change during the acceleration pulse and $L_o$ is the inductance of the magnet (with the projectile in place) before the test. In either case greater efficiency is realized when $L_o$ is lowered. In Equation 5 a maximum of nearly 50 percent efficiency occurs as $L_o$ approaches zero. Also efficiency is lowered by the $I^2R$ energy losses occurring in both the primary circuit and the projectile. In Reference 2, it is shown that the power loss occurring in a plane conductor is given by the expression:

$$W_L = \frac{1}{2} R_s |\bar{J}_2|^2 \qquad (7)$$

where $\bar{J}_2$ is the surface current density expressed in amperes/meter width and

$$R_s = \sqrt{\frac{\pi f \mu}{\sigma}} \qquad (8)$$

Therefore, since the power loss is inversely proportional to the square root of the conductivity, a projectile of higher conductivity will consume less power with a given magnetic field.

If the operating conditions are such that 1) the time duration of the acceleration pulse is constant and 2) the magnetic field density B, is proportional to the current flow in the magnet, the force, energy and efficiency expressions are easily obtained. With reference to Equation 1, the peak force, or acceleration, is proportional to the square of the magnetic field density. When magnetic field density B is proportional to the current flow in the magnet, which in turn is proportional to the capacitor bank voltage, the magnetic field density B is proportional to the capacitor bank voltage. With the above-stated conditions, the accelerating force may be expressed as proportional to the square of the capacitor bank voltage as follows:

$$F = K_F V^2 \qquad (9)$$

where F is the accelerating force, $K_F$ is a constant and V is the capacitor bank voltage. From kinematics, for a constant time duration, the kinetic energy is proportional to the square of the accelerating force. Therefore

$$KE = K' (F)^2 = K_{KE} V^4 \qquad (10)$$

where KE is the kinetic energy of the projectile and K' and $K_{KE}$ are constants. The potential energy stored on the capacitor bank is proportional to the square of the voltage and is given by

$$PE = \frac{1}{2} CV^2 \qquad (11)$$

where C is the total capacitance of the bank. By defining the efficiency, $\epsilon$, as the ratio of kinetic energy to potential energy, the efficiency is then proportional to the square of the capacitor bank voltage.

$$\epsilon = \frac{KE}{PE} = K_\epsilon V^2 \qquad (12)$$

The maximum kinetic energy of the system is limited by the analysis of H. P. Furth as expressed in Equations 5 and 6. In practice, the conditions stated to develop the fourth power relationship between kinetic energy and capacitor bank voltage will be realized when the inductance change, created by projectile displacement, is small compared to the initial inductance of the system when the projectile is in place. Equations 5 and 6 show that the small inductance change will yield a low efficiency.

## Instrumentation

As mentioned previously, the signal from the accelerometers is recorded directly and is not filtered. Input to the magnet is monitored by measuring the current flow in the magnet. Magnet output is determined by measuring the field strength. Current flow is measured with a current-viewing resistor in series with the magnet. Field strength is measured by integrating the output of a pickup coil placed in the center of the magnet (Reference 3). Field strength against the projectile is a function of the volume between the magnet and the projectile and is not the same as the field strength in the center of the coil. Equation 4 shows that if the inductance remains constant, the current and field strength would have the same signature. Therefore, if both the current and field strength are monitored, the difference in waveforms will reflect the time-varying inductance change. This is shown in Figure 7. The flux $\phi$ represents an integrated pickup coil in the center of the magnet. Both the current and the accelerating force peak at nearly the same time and before the flux peaks.

As stated earlier, the acceleration force is monitored by a crystal accelerometer. It is significant that the projectile serves as a magnetic shield for the accelerometer, preventing an enormous signal (because of the field) from reaching the accelerometer. The effect of induced noise was

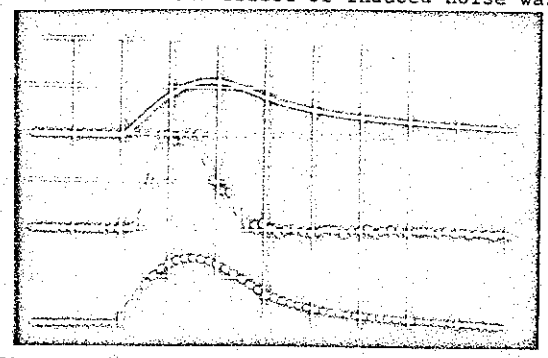

Time ⟶ (50 μsec/cm)

Top Trace - Magnetic Flux $\phi$

Middle Trace - Force

Bottom Trace - Magnet Current

Figure 7. Field-Current-Force Relationship

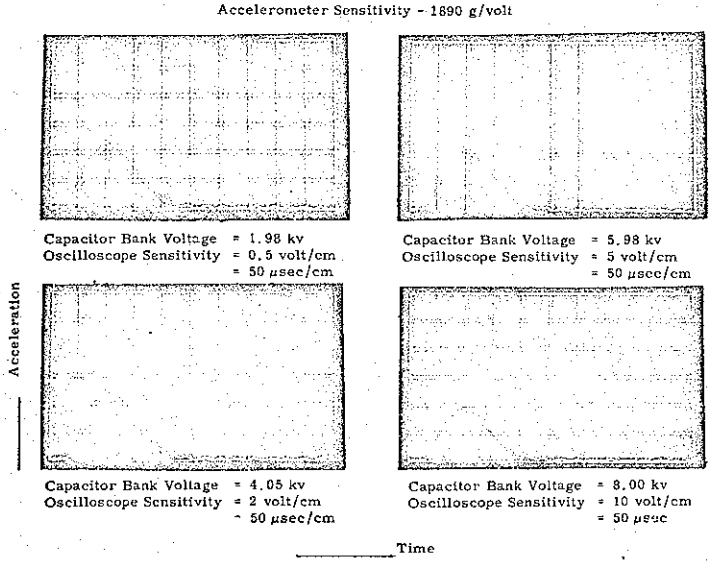


Figure 8. Unfiltered Acceleration Pulses at Various Capacitor Bank Voltages Using 30-Turn Coil

TABLE 1

Data Tabulated from Figure 8

Calibration - 1890 g/volt

Projectile and Accelerometer Weight - 0.33 pounds

| Test No. | Capacitor Bank Voltage (kv) | Peak Acceleration (g) | Peak Force (lbs) | Final Velocity (fps) | Projectile Kinetic Energy (ft-lb) | Capacitor Bank Potential Energy (ft-lb) | Energy Efficiency KE/PE (%) |
|---|---|---|---|---|---|---|---|
| 1 | 1.98 | 2,300 | 760 | 7.66 | 0.25 | 173 | 0.17 |
| 2 | 4.05 | 9,150 | 3,020 | 28.3 | 4.45 | 724 | 0.56 |
| 3 | 5.98 | 19,200 | 6,360 | 60.5 | 18.5 | 1,580 | 1.17 |
| 4 | 8.0 | 34,500 | 18,400 | 100.8 | 51.4 | 2,830 | 1.81 |

TABLE 2

Data Tabulated from Figure 11

Calibration - 660 g/volt

Projectile and Accelerometer weight - 1.96 pounds

| Test No. | Capacitor Voltage (kv) | Accelerometer Output (volts) | Peak Acceleration (g) | Peak Force (lbs) | Velocity Final (fps) | Projectile Kinetic Energy (ft-lb) | Stored Capacitor Potential Energy (ft-lb) | Energy Efficiency KE/PE (%) |
|---|---|---|---|---|---|---|---|---|
| 1 | 2 | 2.7 | 1,780 | 3,500 | 4.6 | 0.64 | 177 | 0.36 |
| 2 | 4 | 11 | 7,270 | 14,300 | 18.6 | 10.5 | 707 | 1.5 |
| 3 | 6 | 25 | 16,500 | 32,400 | 42.3 | 54.4 | 1,590 | 3.42 |
| 4 | 8 | 44 | 29,000 | 57,000 | 74.4 | 168 | 2,830 | 5.94 |

checked by duplicating the entire accelerometer data acquisition system, except that the accelerometer was suspended about 1/8 inch below an aluminum disc 2 inches in diameter and 1 inch thick, which was mounted against the coil. The 1/8-inch distance was chosen to allow the magnetic field (resulting from the capacitor bank discharge) to pass its peak value before the projectile struck the accelerometer. The induced noise was about 1 percent of the accelerometer output which would be expected had the accelerometer been mounted directly to the projectile.

## Test Results and Conclusions

Oscilloscope readings obtained using a 30-turn pancake coil and an aluminum projectile 2 inches in diameter and 1 inch thick are shown in Figure 8. The high frequency component accompanying the primary acceleration pulse is attributed to mechanical noise in the projectile. The data from Figure 8 are tabulated in Table 1. For this particular series the capacitor bank voltage was limited to a 4-to-1 increase (from 2 kv to 8 kv) so that the maximum percentage of inductance change created by projectile displacement would be of the order of 1 or 2 percent of the initial inductance of the system. Since the inductance change is low, it is expected that Equations 9, 10, and 12 would be valid. The evaluation of the constants of Equations 9, 10, and 12 yield the following results:

$$\text{Force} = 183\ (V_c)^2 \qquad (13)$$

$$\text{Kinetic Energy} = .015\ (V_c)^4 \qquad (14)$$

$$\text{Efficiency} = .035\ (V_c)^2 \qquad (15)$$

where $(V_c)$ represents the capacitor bank voltage in kilovolts. The constants of both Equations 13 and 15 are within ± 8 percent and the constant of Equation 14 is within ± 15 percent. The tolerances quoted are within the experimental error of the system. The plots of the acceleration, kinetic energy, and efficiency tabulated in Table 1 are shown graphically in Figure 9.

The repeatability of the electromagnetic shock facility is demonstrated by the oscilloscope recordings in Figure 10. These data were obtained by repeated tests at the same capacitor bank voltage. The amplitude of these three pulses was essentially the same and was well within the accuracy of the capacitor bank voltage.

The oscilloscope readings of Figure 11 were obtained with a magnet similar to the magnet used for Figure 8. However, the data shown in Figure 11 and tabulated in Table 2 were obtained using an aluminum disc 3-1/2 inches in diameter and 2 inches thick. The peak accelerometer output was estimated and refers to the amplitude of the primary pulse rather than the mechanical noise accompanying the pulse.

A larger diameter projectile will effect a larger inductance change for a given projectile displacement. Therefore, it would be expected that

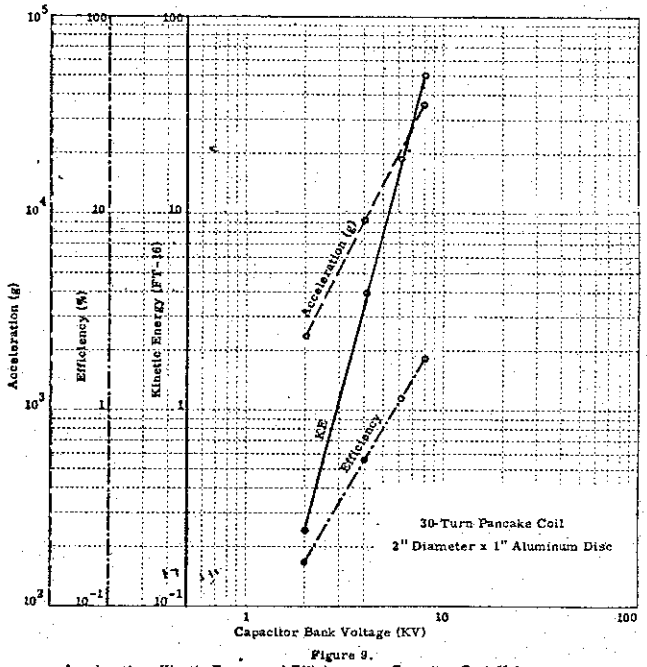


Figure 9.
Acceleration, Kinetic Energy and Efficiency vs. Capacitor Bank Voltage (Data from Table 1)

the larger diameter projectile would be more efficient. A comparison between Tables 1 and 2 of the efficiency values shows this to be true. The penalty of the higher efficiency is that the acceleration pulse changes shape as the input energy is increased. Although the time duration of the acceleration pulse is approximately constant, the peak acceleration occurs sooner as the capacitor bank voltage is increased. The decrease of the time until peak acceleration occurs is due to the greater projectile displacement, for a given amount of time, during the higher efficiency test. At the greater distance the influence of the magnetic field will be decreased; therefore, the acceleration peak will occur earlier.

From the data of Table 2, the constant of Equation 13 is $K_F = 890 \frac{\text{lbs force}}{(V_c)^2}$ within ± 3 percent. As expected, the force constant $K_F$ increases as the projectile diameter increases. The ± 3 percent obtained from the data of Table 2 suggests that the squared relationship between the force and voltage is less critical than would be expected. This may be attributed to the fact that a practical system tends to be self-compensating, i.e., as the projectile moves away the pulse time tends to decrease, but the inductance increases and this increases the duration of the magnetic field which in turn tends to increase the pulse time.

A comparison of the wave forms of Figure 8 and Figure 11 shows that the signal-to-noise ratio remained constant on the data of Figure 8 but decreased on the recordings of Figure 11. The decrease in signal-to-noise ratio is attributed to the mechanical resonant system being more sensitive to the sharper rise time of the higher energy pulses.

Figure 12 shows oscilloscope recordings made

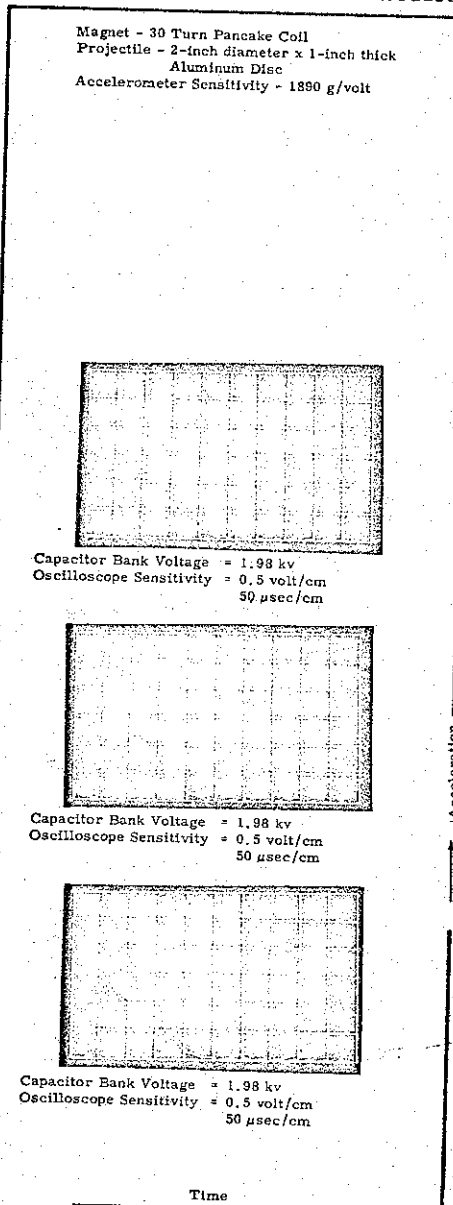


Figure 10. Unfiltered Acceleration Pulses at Same Capacitor Bank Voltages

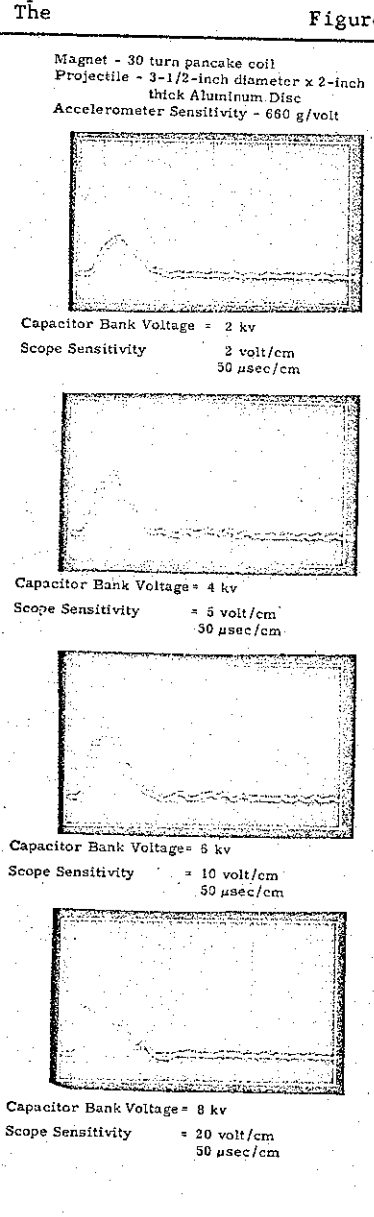


Figure 11. Unfiltered Acceleration Pulses at Various Capacitor Bank Voltages

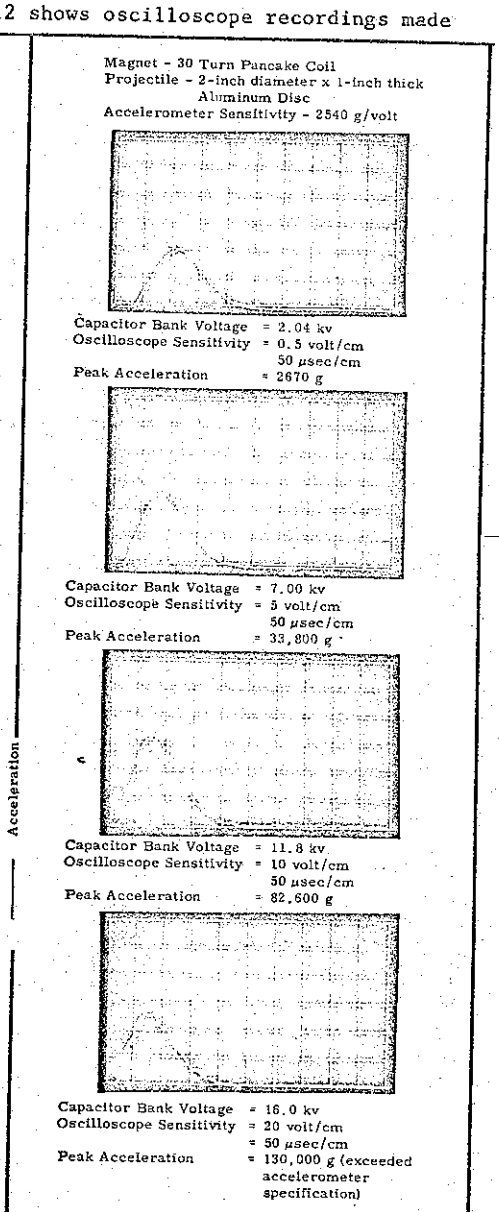


Figure 12. Unfiltered Acceleration Pulses Over Wide Range of Capacitor Bank Voltages Using 30-Turn Coil

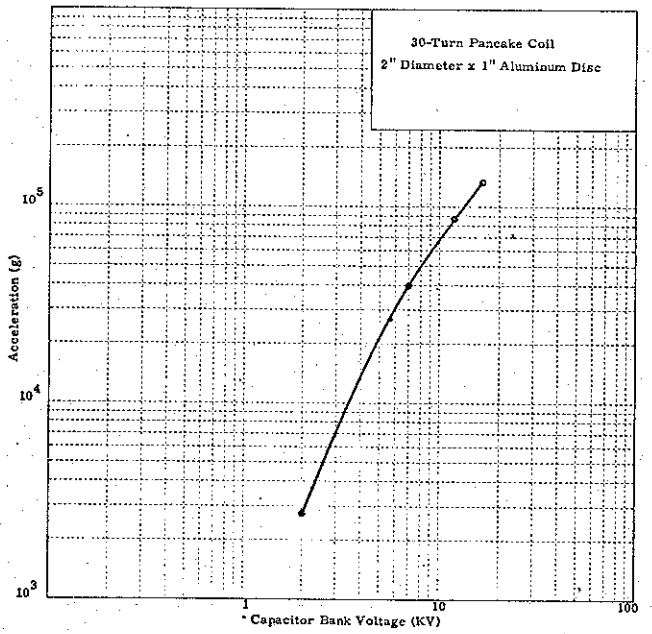


Figure 13.
Acceleration vs. Capacitor Bank Voltage
(Data from Figure 12)

with a wide range of capacitor bank voltages. A 30-turn pancake coil and an aluminum disc 2 inches in diameter and 1 inch thick were used for this test. The acceleration versus capacitor bank voltage is plotted in Figure 13. The capacitor bank voltage was varied between 2 kv and 16 kv which increases the potential energy by 64. The indicated acceleration was between 2670 g and 130,000 g. (The accelerometer was rated to 100,000 g; however, basic sensitivity before and after the test was the same.) With the 2-inch diameter projectile the acceleration signature remained reasonably constant throughout the test series. Also, the acceleration versus voltage curve is smooth, although nonlinear, on the log-log graph.

Figures 14, 15, and 16 show data obtained with 100-turn, 200-turn, and 300-turn coils, respectively. These recordings show both the field strength, $\emptyset$, which is the top trace, and the acceleration pulse, which is the bottom trace. The field strength $\emptyset$ was recorded to demonstrate the smooth forcing function provided by the magnetic field. In each case, an aluminum disc projectile 3-1/2 inches in diameter and 1 inch thick was used. Since the higher inductance coils decrease the frequency of the capacitor bank discharge, longer acceleration pulse times are obtained. A longer pulse time corresponds to an amplitude decrease, as would be expected. For instance, at 10 kv, the 100-turn coil produces a 22,000-g acceleration pulse with approximately a 0.5-millisecond time duration, while the 300-turn coil produces a 7740-g pulse with approximately a 1-millisecond time duration. Also, for the higher inductance coils, the higher the input energy, the shorter the acceleration pulse rise time and pulse duration. This decrease in pulse rise time is attributed to the decrease in magnetic field intensity at the greater distances, as explained earlier. In addition, the acceleration pulse goes below zero on the low level tests with the 200- and 300-turn coils. At the time of this writing, the negative undershoot is believed to be due to the RC time constant of input circuit to the cathode follower. As the pulse times grow shorter, the low RC time constant has less effect.

Figure 17 shows the plots of the acceleration versus capacitor bank voltage for the data of Figures 14, 15, and 16. From the graph it can be seen that the higher the number of turns, which corresponds to higher inductance, the more nonlinear the acceleration amplitude appears on the log-log plot. The roll-off of the 300-turn coil acceleration plot indicates that the magnetic field attenuation versus distance was greater than that of the lower inductance coils.

## Limitations

### Force Amplitude

There is virtually no limit on the maximum or minimum force available from transient magnetic fields. Controlled experiments have been conducted where magnetic pressures, in limited volumes, of well over 100,000 psi have been generated (Refer-

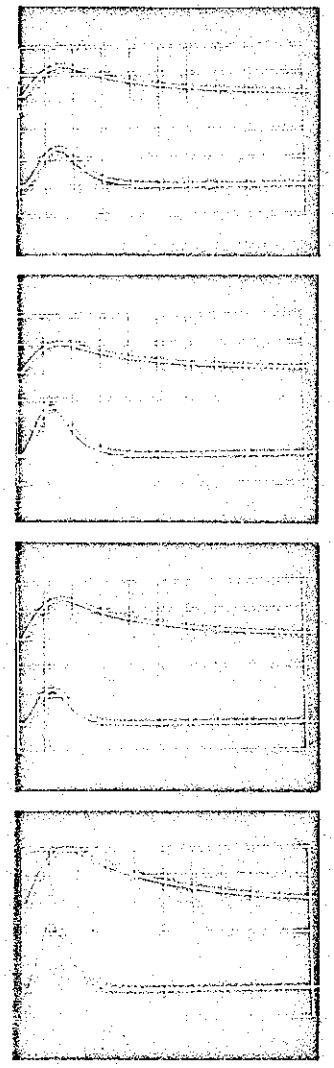


Figure 14. Unfiltered Acceleration Pulses and Field Strength at Various Capacitor Bank Voltages Using 100-Turn Coil

ence 1). The primary limitation of a system is the ability of the magnet to survive the combination of mechanical forces and electrical breakdown. The high field density in the magnet core exerts a high radial compressive stress on the windings at the same time as the magnet receives the axially compressive load (Reference 3). The mechanical strain promotes a turn-to-turn electrical breakdown that constitutes a coil failure. In general, the ability of the magnet to withstand failure depends on the type of magnet used. The 30-turn magnets currently being used at Sandia Corporation have operated with field strengths in excess of 100,000 gauss (which corresponds to 5600 psi) in the center of the coil without failure. In some cases it could be practical to design coils for one-shot operation. Although the magnet may fail, the inertial effects will aid in holding the magnet together during the actual time of the acceleration pulse.

## Force Width

Before crowbar occurs, the discharge circuit is merely an underdamped R-L-C circuit. Therefore, the rise time of the acceleration pulse can be changed by varying the inductance or capacitance of the circuit. As demonstrated in this report, the pulse time can readily be varied by a factor of 10. The pulse time could be increased still further with a corresponding reduction in amplitude. With the existing equipment at Sandia Corporation, it is believed that pulse times of greater than 10 milliseconds, with corresponding reductions in amplitude, could be obtained. A minimum pulse time of approximately 10 microseconds can be obtained with standard components by using less capacitance and/or lower inductance magnets. The trailing edge of the acceleration pulse may be determined by the L/R time constant of the crowbarred circuit. This may be varied, over a limited range, by merely changing the time constant.

## Cost

The initial investment for a capacitor bank is relatively high. A complete system could be fabricated for approximately 30 cents/joule, depending on size, using standard components. The high initial cost is offset by the negligible operating costs.

Magnet - 200-Turn Flat Circular Coil
Projectile - 3-1/2-inch diameter x 1-inch thick Aluminum Disc
Accelerometer Sensitivity - 1720 g/volt

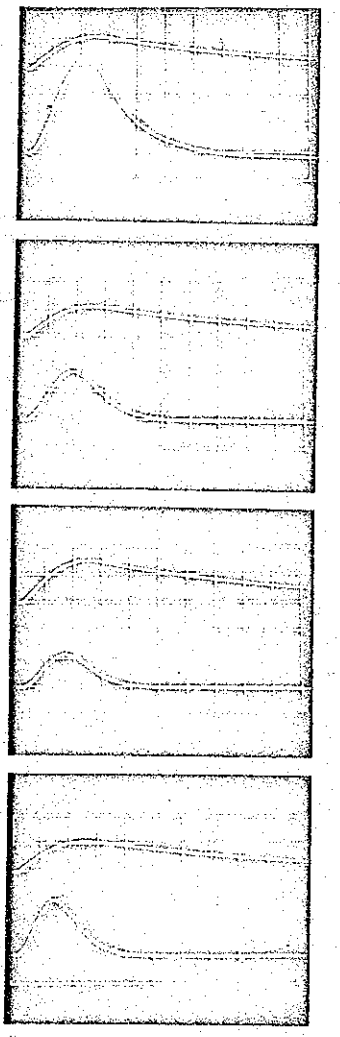

Capacitor Bank Voltage = 2.01 kv
Oscilloscope Sensitivity
Field Strength ∮ = 0.2 volt/cm
Acceleration = 0.2 volt/cm, 200 μsec/cm
Peak Acceleration = 1140 g

Capacitor Bank Voltage = 4.95 kv
Oscilloscope Sensitivity
Field Strength ∮ = 0.5 volt/cm
Acceleration = 2 volt/cm, 200 μsec/cm
Peak Acceleration = 5800 g

Capacitor Bank Voltage = 7.00 kv
Oscilloscope Sensitivity
Field Strength ∮ = 0.5 volt/cm
Acceleration = 5 volt/cm, 200 μsec/cm
Peak Acceleration = 9800 g

Capacitor Bank Voltage = 9.98 kv
Oscilloscope Sensitivity
Field Strength ∮ = 1.0 volt/cm
Acceleration = 5 volt/cm, 200 μsec/cm
Peak Acceleration = 16,340 g

Acceleration
Time

Figure 15. Unfiltered Acceleration Pulses and Field Strength at Various Capacitor Bank Voltages Using 200-Turn Coil

Magnet - 300-Turn Flat Circular Coil
Projectile - 3-1/2-inch diameter x 1-inch thick Aluminum Disc
Accelerometer Sensitivity - 1720 g/volt

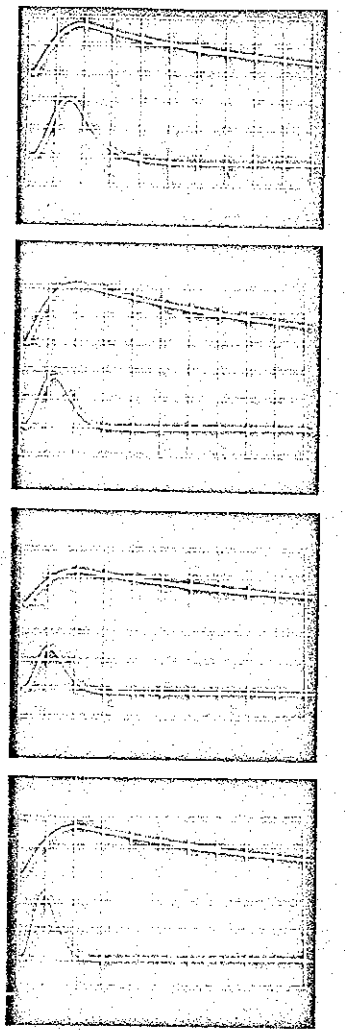

Capacitor Bank Voltage = 2.00 kv
Oscilloscope Sensitivity
Field Strength ∮ = 0.1 volt/cm
Acceleration = 0.2 volt/cm, 500 μsec/cm
Peak Acceleration = 688 g

Capacitor Bank Voltage = 5.00 kv
Oscilloscope Sensitivity
Field Strength ∮ = 0.2 volt/cm
Acceleration = 1.0 volt/cm, 500 μsec/cm
Peak Acceleration = 3060 g

Capacitor Bank Voltage = 7.02 kv
Oscilloscope Sensitivity
Field Strength ∮ = 0.5 volt/cm
Acceleration = 2.00 volt/cm, 500 μsec/cm
Peak Acceleration = 4990 g

Capacitor Bank Voltage = 10.0 kv
Oscilloscope Sensitivity
Field Strength ∮ = 0.5 volt/cm
Acceleration = 2.00 volt/cm, 500 μsec/cm
Peak Acceleration = 7740 g

Acceleration
Time

Figure 16. Unfiltered Acceleration Pulses and Field Strength at Various Capacitor Bank Voltages Using 300-Turn Coil

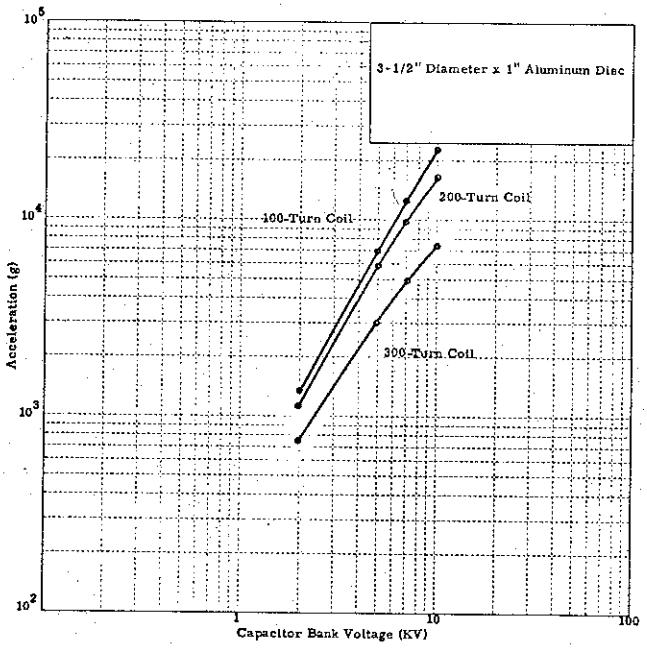


Figure 17.
Acceleration of Various Coils vs. Capacitor Bank Voltage
(Data from Figures 14, 15, and 16)

## Summary

Transient magnetic fields are readily capable of producing high-energy acceleration pulses. These acceleration pulses are controllable, repeatable, predictable, and free from mechanical noise in the high-g range. Although the technique could be applied throughout the range of 10 microseconds to 10 milliseconds, it is particularly competitive throughout the microsecond range. The ease of operation and negligible operating costs offset the high initial cost of a capacitive energy storage facility.

## Appendix A

### Field Analysis

Referring to Figure A1, consider a sheet of oscillating current flowing into the paper in the vicinity of a conductor. Let the current sheet and the conductor be very wide so that the edge effects may be neglected. This current sheet gives rise to a magnetic field around itself. In the air gap between the coil and the conductor, the magnetic field is represented by the magnetic intensity vector $\bar{H}_o$. The time varying magnetic field will induce a current flow in the conductor at the frequency of the magnetic field. The magnitude of the current decreases exponentially versus the depth of penetration into the conductor.

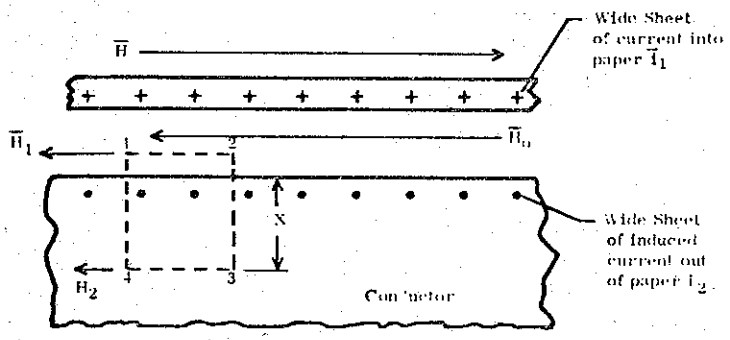


Figure A1. Basic Current-Field/Induced-Current Relationship

Ampere's Circuital Law is applied (Reference 4) around path 1-2-3-4 to analyze the magnetic field intensity existing within the conductor. The total current enclosed may be expressed as the average current density times the conductor area enclosed by path 1-2-3-4. This is expressed as follows:

$$\oint_{1\text{-}2\text{-}3\text{-}4} \bar{H} \cdot d\bar{\ell} = I = \left(\bar{i}_{2avg}\right) \cdot \left(\bar{A}rea_c\right) \qquad (1A)$$

In Equation 1A, $\bar{H}$ is the magnetic intensity vector in amperes/meter, $\bar{\ell}$ is the length in meters, I is the total current enclosed by the path, $\bar{i}_{2avg}$ is the average current density expressed in amperes/meters$^2$, and $\bar{A}rea_c$ is the enclosed conductor area. Since all field contributions are parallel to the conductor surface, field contributions along paths 2-3 and 4-1 are zero, and Equation 1A is evaluated as follows:

$$\left(H_{1\text{-}2}\right)\left(\ell_{1\text{-}2}\right) + \left(H_{3\text{-}4}\right)\ell_{3\text{-}4} = \left(i_{2avg}\right)\left(Area_c\right) \qquad (2A)$$

Therefore:

$$\left(-H_1 + H_2\right)\Delta\ell = \left(i_{2avg}\right)\left(Area_c\right)$$

$$H_1 - H_2 = -\frac{\left(i_{2avg}\right)\left(Area_c\right)}{\Delta\ell}$$

$$= -i_{2avg}\,(X) \qquad (3A)$$

In Equation 3A, x is the length of the path, normal to the surface, contained in the conductor and measured in meters. Equation 3A is a generalized expression for the attenuation of field intensity through the conductor in terms of the current distribution in the conductor. There are no restrictions on the location of the path around which the integration is to be performed. Therefore, if path length 1-2 is allowed to be outside the conductor, as shown in Figure A1, the value of $\bar{H}_1$ becomes $\bar{H}_o$, which is the magnetic intensity vector existing in the air gap.

Now, consider the effect of allowing path lengths 2-3 and 4-1 to shrink to an infinitely small length so that the entire path is contained within the conductor. The average current density then becomes the value of the current density. Thus from Equation 4, the following equation results:

$$H_1 - H_2 = \Delta H = -i_2\Delta X \qquad (4A)$$

Expressed in differential form, this becomes:

$$i_2 = -\frac{dH}{dX} \qquad (5A)$$

For simplicity, the vector notation has been dropped during the evaluation of Equation 1A. However, the direction of current flow may be determined by the right hand rule. Therefore, at any point within the conductor, the current density is equal to the negative rate of change of field intensity with respect to distance into the plate.

Magnetic Field Force

To determine the force exerted on the conductor, the force relationship existing between a current flow and a magnetic field is applied. In terms of current density, the force expression (Reference 5) per unit volume is given by:

$$\frac{d\bar{F}}{dV} = \bar{i} \times \bar{B} \qquad (6A)$$

where V is the volume in the conductor.

The magnetic flux density vector $\bar{B}$, expressed in webers/meter$^2$ is given by:

$$\bar{B} = \mu\bar{H} \qquad (7A)$$

Combining Equations 5A, 6A, and 7A, the force per unit volume is given by:

$$\frac{d\bar{F}}{dV} = \bar{i} \times \bar{B} = \frac{1}{2\mu}\frac{dB^2}{dX}\bar{a} \qquad (8A)$$

where $\bar{a}$ is a unit vector normal to the conductor surface and directed into the conductor.

Since the magnetic flux density is constant throughout any plane parallel to the conductor surface, Equation 8A may be expressed as a force per unit area, which is called the magnetic pressure $\bar{p}$.

Therefore:

$$\bar{p} = \frac{B^2}{2\mu}\bar{a} \qquad (9A)$$

Equation 9A is the expression, in rationalized mks units, for the "magnetic pressure", expressed in newtons/meter 2, exerted on a conductor in the presence of a time-varying magnetic field. The vector $\bar{B}$ is the magnetic flux density existing at the surface of the conductor. The validity of this equation rests on the fact that the current induced in the conductor prevents the field from leaking through the conductor. It can be shown that if the skin depth of the current is comparable to the conductor thickness so that the field appears on the opposite side, the current is decreased, resulting in less pressure on the conductor. This reaches a limit when the field on both sides is equal, resulting in no induced current and zero force.

Several sets of units are available and are in use to describe electromagnetics. Up to this point only rationalized mks units have been used in this report to remain consistent with most tests on this subject. In practice, however, Gaussian or unrationalized cgs units are used more extensively. Equation 9A would thus be modified to

$$\bar{p} = \frac{B^2}{8\pi}\bar{a} \qquad (10A)$$

where

$\bar{p}$ = magnetic pressure in dynes/cm$^2$

B = magnetic flux in gauss

Several recent publications are helpful in understanding theory and uses of magnetic pressure. Reference 6 presents a rigorous and thorough approach to the theory of magnetic forces and energies and the analogy between a magnetic field and a gas.

Appendix B -- Circuit Theory

Figure B1 represents a circuit consisting of an underdampened series RLC primary and a secondary consisting of a series RL circuit inductively coupled to the primary. The capacitor, C, is initially charged to a voltage, V. When the switch is closed, primary current, $i_1$, induces a current flow in the secondary, $i_2$. The secondary then receives an acceleration force away from the primary. If the secondary circuit (the projectile) is unrestrained, the resulting displacement forms a changing mutual inductance. By applying conventional circuit theory and the conservation of energy, it can be shown (Reference 7) that the accelerating force is given by:

$$f = -i_1\, i_2 \frac{\partial M}{\partial x} \qquad (1B)$$

where $i_1$ = instantaneous primary current in amperes

$i_2$ = instantaneous secondary current in amperes

M = instantaneous mutual inductance in henrys

x = displacement in meters

f = force in newtons

The force of acceleration will always tend to separate the two circuits regardless of the initial voltage polarity or direction of primary current flow.

Appendix C -- Field Energy Theory

The energy density contained in a magnetic field is expressed (Reference 8) by:

$$w_{fld} = \frac{1}{2}\frac{B^2}{\mu} \qquad (1C)$$

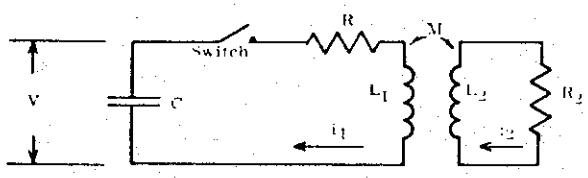


Figure B1

where $w_{fld}$ = energy density in Joules/meter$^2$

$B$ = flux density in Webers/meter$^2$

$\mu$ = permeability in rationalized mks units.

The total energy in a given field is then obtained by integrating Equation 1C over the desired volume as follows:

$$W_{fld} = \int_v \frac{1}{2} \frac{B^2}{\mu} dv. \qquad (2C)$$

The force available from the field may be expressed as the rate of change of energy with respect to distance when the flux is held constant. Consider an incremental volume, dv, as shown in Figure C1, consisting of an incremental cross sectional area dA and a depth of dX such that

$$dv = dA\ dx \qquad (3C)$$

Let the incremental volume contain a uniform magnet flux density, B. In general, a force may be expressed as the rate of change of energy with respect to distance. Therefore, the force, expressed in terms of magnetic flux density, is given as:

$$F = -\frac{dW}{dX}_{\phi=\text{constant}} = -\frac{d}{dx} \int_v \frac{1}{2} \frac{B^2}{\mu} dv. \qquad (4C)$$

If dy is unity, then

$$\phi = BA = B\ dy\ dx = B\ dx. \qquad (5C)$$

Equation 4C is then evaluated as follows:

$$F_{\phi = \text{constant}} = -\frac{d}{dx} \int_v \frac{1}{2\mu} \frac{\phi^2}{(dx)^2} dA\ dx \qquad (6C)$$

$$= -\int_A \frac{1}{2\mu} \frac{\phi^2}{(dx)^2} dA = -\frac{1}{2\mu} \frac{\phi^2}{(dx)^2} A$$

$$= -\frac{1}{2\mu} B^2 A .$$

where $\phi$ is the total flux enclosed in the volume. The negative sign indicates that the force is a function of decreasing field energy.

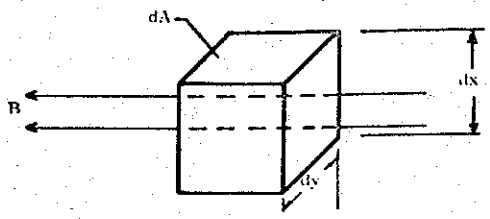


Figure C1


Acknowledgements

Mr. Kenneth D. Marx, Sandia Corporation, Livermore Laboratory, Test Design Division 8121, who, together with the author, developed the original idea.

Dr. H. P. Furth, Lawrence Radiation Laboratory, Livermore, for suggesting the basic approach and for assistance in theoretical aspects.

Mr. D. H. Birdsall, Lawrence Radiation Laboratory, Livermore, for construction ideas and hardware.

Mr. A. R. Harvey, Lawrence Radiation Laboratory, Livermore, for coil design and fabrication.


References


1. Edited by Kolm, H.; Lax, B.; Bitter, F.; and Mills, R.; High Magnetic Fields, MIT Press and John Wiley and Sons, 1962, Chapter 22 "Pulsed Magnets" by Furth, H. P.

2. Ramo, S. and Whinnery, J. R., Fields and Waves in Modern Radio, 2nd Edition, John Wiley and Sons, New York, 1953, Chapter 6.

3. Furth, H. P. and Waniek, R. W., "Production and Use of High Transient Magnetic Fields I," Review of Scientific Instruments, Vol. 27, No. 4, April 1956, pp. 195-203.

4. Rogers, W. E., Electric Fields, McGraw-Hill Book Company, New York, 1954, Chapter 9.11.

5. Hayt, Jr., W. H., Engineering Electromagnetics, McGraw-Hill Book Company, New York, 1958, Chapter 9.2.

6. Birdsall, D. H.; Ford, F. C.; Furth, H. P.; and Riley, R. E.; "Magnetic Forming," American Machinist, Vol. 105, No. 6, March 20, 1961.

7. Lathan, B. F. and Radnik, J. L., Electromagnetic Projector Study, Armour Research Foundation, April 1961.

8. Fitzgerald, A. E. and Kingsley, C., Electric Machinery, McGraw-Hill Book Company, New York, 1952, Chapter 2.